

## Turbulent boundary layers up to $Re_\theta=2500$ studied through simulation and experiment

P. Schlatter,<sup>a)</sup> R. Örlü, Q. Li, G. Brethouwer, J. H. M. Fransson, A. V. Johansson, P. H. Alfredsson, and D. S. Henningson  
 Linné Flow Centre, KTH Mechanics, SE-100 44 Stockholm, Sweden

(Received 4 March 2009; accepted 24 April 2009; published online 20 May 2009)

Direct numerical simulations (DNSs) and experiments of a spatially developing zero-pressure-gradient turbulent boundary layer are presented up to Reynolds number  $Re_\theta=2500$ , based on momentum thickness  $\theta$  and free-stream velocity. For the first time direct comparisons of DNS and experiments of turbulent boundary layers at the same (computationally high and experimentally low)  $Re_\theta$  are given, showing excellent agreement in skin friction, mean velocity, and turbulent fluctuations. These results allow for a substantial reduction of the uncertainty of boundary-layer data, and cross validate the numerical setup and experimental technique. The additional insight into the flow provided by DNS clearly shows large-scale turbulent structures, which scale in outer units growing with  $Re_\theta$ , spanning the whole boundary-layer height. © 2009 American Institute of Physics. [DOI: 10.1063/1.3139294]

The study and understanding of the turbulent flow close to solid walls are a major topic in today's research in fluid dynamics. Although in nature or technical applications the surfaces are usually curved, possibly rough, and the mean flow is seldom exactly two dimensional, the spatially developing, zero-pressure gradient turbulent boundary layer on a smooth, flat plate is an important canonical flow case for theoretical, numerical, as well as experimental studies. In recent years, particularly careful experiments have been conducted. For instance, Österlund *et al.*<sup>1</sup> performed extensive measurements of mean quantities in the minimum turbulence level (MTL) wind tunnel at KTH Stockholm using hot-wire anemometry and oil-film interferometry for Reynolds numbers  $Re_\theta$  (based on momentum thickness  $\theta$  and free-stream velocity  $U_\infty$ ) ranging from 2530 to 27 300, with five measurement positions below  $Re_\theta=6000$ . Recall that  $Re_\theta$  provides a measure of the streamwise position.

Direct numerical simulation (DNS) of turbulent flows relies on numerically resolving all relevant scales of motion. As the Reynolds number is getting larger the scale separation between the large and smallest scales is increasing considerably, limiting the Reynolds number attainable in DNS to low values compared to experiments. As opposed to turbulent channel<sup>2</sup> and pipe flow,<sup>3</sup> only few numerical results from DNSs of turbulent boundary layers have been performed for medium or high (computational) Reynolds numbers. The main reason is the extreme cost of spatial DNS due to the long and consequently wide and high domains required, and the loss of one homogeneous direction. Spalart's simulations<sup>4</sup> using an innovative spatiotemporal approach provided valuable data at  $Re_\theta=300, 670, 1410$ , which have become a standard reference for numerical boundary-layer data. Komminaho and Skote<sup>5</sup> performed a spatial DNS up to  $Re_\theta=700$ . The highest Reynolds number reached in DNS to date is the data reported by Ferrante and Elghobashi<sup>6</sup> at

$Re_\theta=2900$ , however, obtained in a comparably short computational domain in which the turbulence, in particular, the large-scale structures, may not be fully developed. Either the computational approaches were too different to the experiments or the Reynolds numbers were too low to make possible a robust comparison.

For turbulent boundary layers, the Reynolds number  $Re_\theta \approx 2500$  has to be considered at present high from a DNS point of view. On the other hand, a high-quality boundary layer can be hard to establish and accurately measure at such  $Re_\theta$ , since low Reynolds number boundary-layer experiments need to be carried out at low velocities and for small distances from the leading edge. In the case of hot-wire measurements accurate calibration at low velocities is needed especially for the near-wall measurements, whereas the choice of tripping may affect the onset of transition to turbulence. The latter will affect the structure of the turbulence mainly in the outer part, leading to influences in the turbulent statistics. Near the leading edge a pressure gradient is unavoidable, but can be reduced to nearly zero by adjusting the geometry of the setup. Turbulent boundary-layer data available in literature have usually been taken in a range of  $Re_\theta$  by varying the free-stream velocity. The pressure gradient has often been tuned for one specific case, since readjustment of the pressure gradient is usually time consuming and therefore not always realized. Thus some of the data available in the literature are not taken in the optimal configuration for the  $Re_\theta$  in question.

Due to the difficulty of both DNS and experiments at Reynolds numbers  $Re_\theta$  on the order of a few thousand, there is a comparably large spread of the existing data in literature, both for integral, mean, and fluctuating turbulent quantities, see, e.g., Ref. 7. There is thus a need for accurate and reliable DNS data of spatially developing turbulent boundary layers with  $Re_\theta$  to be compared to high-quality experimental results. To this end, the inflow in the numerical simulation should be positioned far enough upstream, i.e., comparable to where natural transition occurs, to ensure that the flow

<sup>a)</sup>Electronic mail: pschlatt@mech.kth.se.

reaches a fully developed, undisturbed equilibrium state further downstream.

The present letter reports a combined experimental and numerical study of zero-pressure-gradient turbulent boundary layers, aiming to provide a well-validated data set pertaining to the dynamics of the mean and fluctuating turbulent quantities as a function of the downstream distance. Both the experiments and simulations are performed with well established and reliable methods. In addition, by considering the same generic flow case both experimentally and numerically, the sensitivity of the results to the respective method limitations, e.g., surface roughness, tripping technique, pressure gradients, and boundary conditions, etc., can be examined.

The simulations are performed using a fully spectral method to solve the time-dependent, incompressible Navier–Stokes equations.<sup>8</sup> In the wall-parallel directions, Fourier series with dealiasing are used whereas the wall-normal direction is discretized with Chebyshev polynomials. Periodic boundary conditions in the streamwise direction are combined with a spatially developing boundary layer by adding a “fringe region” at the end of the domain. In this region, the outflowing fluid is forced via a volume force to the laminar inflowing Blasius profile, located at  $Re_{\delta_0^*}=450$  based on the inflow displacement thickness  $\delta_0^*$ . A low-amplitude wall-normal trip force causes rapid laminar-turbulent transition shortly downstream of the inlet. The chosen spectral method provides excellent accuracy and dispersion properties as compared to low-order discretizations.

The computational domain is  $x_L \times y_L \times z_L = 3000\delta_0^* \times 100\delta_0^* \times 120\delta_0^*$  with  $3072 \times 301 \times 256$  spectral collocation points in the streamwise, wall-normal, and spanwise directions, respectively. The height and width of the computational domain are chosen to be at least twice the largest 99% boundary-layer thickness, which reaches  $\delta_{99} \approx 45\delta_0^*$  at  $Re_\theta = 2500$ . The grid points are nonequidistantly distributed in the wall-normal direction, with at least 15 collocation points within the region  $y^+ < 10$ . The grid resolution in viscous units is then  $\Delta x^+ \times \Delta y_{\max}^+ \times \Delta z^+ = 17.9 \times 8.6 \times 9.6$ . The streamwise and spanwise resolutions are about a factor of 1.5 lower than in the channel-flow study by Hoyas and Jiménez,<sup>2</sup> however, to ensure adequacy of the chosen grid, we also performed a resolution study based on the same box dimensions, but an increased number of grid points as  $4096 \times 385 \times 480$  showing only insignificant differences. Statistics are sampled over  $\Delta t^+ \approx 24\,000$  viscous time units, or 30 in units of  $\delta_{99}/U_\tau$  at  $Re_\theta = 2500$ . Owing to the high computational cost of the simulations, the code is fully parallelized running on  $\mathcal{O}(1000)$  processors.

The turbulent boundary-layer measurements were performed in the MTL wind tunnel on a 7 m long flat plate at  $x=1.6$  m from the leading edge, where the ceiling of the tunnel was adjusted for each measurement run to obtain zero-pressure-gradient conditions. The setup is similar to that of Österlund.<sup>9</sup> The free-stream velocity was 12.0 m/s and the streamwise velocity component was measured by means of hot-wire anemometry using a single wire probe. The sensor length was 0.50 mm, corresponding to about 15 viscous length units. This is sufficiently small in order not to observe effects of spatial averaging on the measured fluctuation lev-

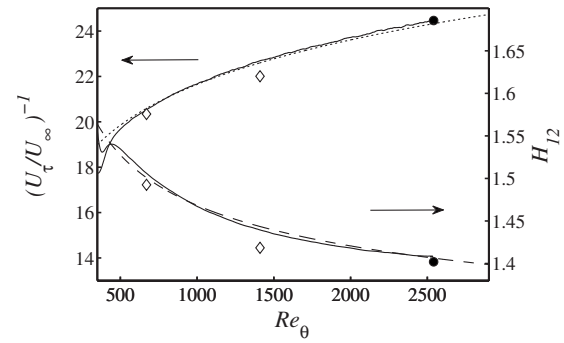


FIG. 1. Skin friction  $U_\tau/U_\infty = \sqrt{c_f/2}$  and shape factor  $H_{12}$  as a function of  $Re_\theta$ . (—) Present DNS, (●) present experimental measurements. (◇) DNS by Spalart (Ref. 4). (⋯)  $c_f = 0.024 Re_\theta^{(-1/4)}$  (Ref. 12), (---) correlation for  $H_{12}$  based on the composite profile suggested by Monkewitz *et al.* (Ref. 13).

els in the near-wall region.<sup>10</sup> A three-dimensional deterministic surface roughness in combination with sandpaper was used to trip the boundary layer in order to obtain a fixed transition point. The skin friction was measured directly and independent from the hot-wire measurements using oil-film interferometry.<sup>11</sup>

The focus of the results presented here is on showing averaged quantities and the fluctuations around that mean value. The considered case consists of a statistically two-dimensional boundary layer evolving in  $x$  and  $y$ , statistically homogeneous in the spanwise direction  $z$  and stationary in time  $t$ . The Reynolds decomposition  $u = \langle u \rangle + u' = U + u'$  is used, the brackets indicating the average in  $z$  and  $t$ . Based on the mean velocity profile  $U(x, y)$  the shear stress at the wall is obtained as  $\tau_w(x) = \mu(dU/dy)|_{y=0}$ . Following the classical theory of turbulent boundary layers, the friction velocity  $U_\tau \equiv \sqrt{\tau_w/\rho}$  provides the relevant velocity scale throughout the boundary layer, whereas the viscous length scale  $\ell_\star \equiv \nu/U_\tau$  is the characteristic length at least close to the wall. The scaled quantities in wall scaling are thus written as, e.g.,  $U^+ = U/U_\tau$  and  $y^+ = y/\ell_\star$ .

In both the simulation and the experiment, the initially laminar boundary layer is tripped at approximately the same distance from the leading edge in terms of  $Re_\theta$ . Further downstream of the tripping location, fully developed turbulence is established in which the boundary layer reaches an equilibrium state with the local production and dissipation of turbulent kinetic energy balancing each other. In the simulations, the extent of the self-similar region downstream of the tripping can be estimated by considering the von Kármán integral equation relating the local skin friction to the growth of the momentum thickness  $\theta$ . Based on this argument, the useful region in the simulation may be defined as ranging from  $Re_\theta = 550$  to 2500, corresponding to 75% of the total computational domain. The peak skin friction Reynolds number  $Re_\tau = U_\tau \delta_{99}/\nu$  is approximately 900 at  $Re_\theta = 2500$ .

Characteristic mean quantities of the turbulent boundary layer up to  $Re_\theta = 2500$  are shown in Fig. 1. The skin friction is shown as the friction velocity scaled by the free-stream velocity, i.e.,  $U_\tau/U_\infty = \sqrt{c_f/2}$ . Surprisingly, the simple correlation  $c_f = 0.024 Re_\theta^{(-1/4)}$  (Ref. 12) provides an accurate fit to the DNS data for the range of Reynolds numbers considered. The agreement with the new experimental measurement

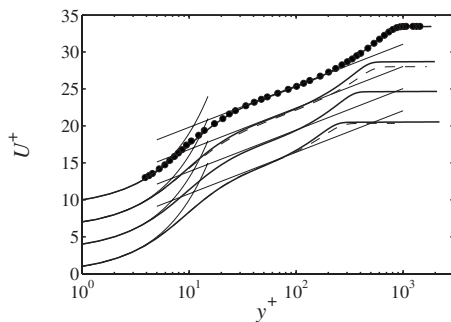


FIG. 2. Mean velocity profile  $U^+$  in viscous units for (—) present DNS at  $Re_\theta=671, 1000, 1412, 2512$ , (●) present measurements at  $Re_\theta=2541$ . (---) DNS by Spalart (Ref. 4) at  $Re_\theta=670, 1410$ . The profiles are shifted by  $U^+=3$  for increasing  $Re_\theta$ . The linear and logarithmic regions are indicated by a thin line, using  $1/\kappa \log y^+ + B$  with  $\kappa=0.41$  and  $B=5.2$ .

point at  $Re_\theta=2500$  is very good. Recall that, experimentally the skin friction is obtained using the oil-film technique<sup>11</sup> independently of the velocity measurements. The shape factor  $H_{12}=\delta^*/\theta$ , i.e., the ratio of displacement to momentum thickness, is also shown; this quantity provides a useful way of characterizing the development state of the boundary layer. It turns out that  $H_{12}$  is a sensitive indicator of the quality of the boundary-layer data at a given  $Re_\theta$ . The agreement with both the new measurements and the shape factor based on the composite velocity profile developed by Monkewitz *et al.*<sup>13</sup> is again satisfactory. Note that the coefficients in the composite profile have been calibrated for experimental boundary layers at higher  $Re_\theta$  than the present one. For comparison, the data points of the DNS by Spalart<sup>4</sup> are also shown in Fig. 1. The skin friction is overpredicted by approximately 5% at the highest  $Re_\theta=1410$ , whereas the shape factor is lower than the data obtained from both the composite profile and the present DNS. This might be a residual effect of the spatiotemporal approach employed.

Profiles of the mean velocity scaled by viscous units  $U^+(y^+)$  obtained from both the present DNS and experiments are shown in Fig. 2. The similarity at the highest Reynolds number shown,  $Re_\theta=2500$ , is excellent. However, there is a discrepancy between the present simulation data and that of Spalart at  $Re_\theta=1410$ , probably due to a suspected lower actual  $Re_\theta$  in the latter simulation. In the wake region and the free stream, Spalart's results agree better with the present data at  $Re_\theta=1000$ . In the near-wall region, all data collapse nicely on the linear relation  $U^+=y^+$ . The von Kármán coefficient  $\kappa$  used to indicate the logarithmic region  $(1/\kappa)\log y^+ + B$  is chosen as  $\kappa=0.41$  which seems to best fit the data at this  $Re_\theta$ . Inspection of the log-law indicator function  $\Xi=y^+(dU^+/dy^+)$  shows that the current DNS velocity profile closely follows the composite profile proposed in Ref. 13 up to  $y^+=100$ . At  $Re_\theta=2500$ , this wall-normal position can approximately be considered as the beginning of the wake region, in which the mean-flow gradient quickly rises to  $\Xi \approx 5.2$  at  $y^+ \approx 600$ . The minimum of  $\Xi$  is at  $y^+ \approx 70$  with a value of  $1/\Xi \approx 0.428$  in good agreement with Ref. 13.

The velocity fluctuations, e.g.,  $u_{\text{rms}}=\sqrt{\langle u'u' \rangle}$ , and the Reynolds shear stress are depicted in Fig. 3 in wall scaling, and compared to the formulations derived from the attached-eddy hypothesis by Marusic and co-workers.<sup>14–16</sup> The agree-

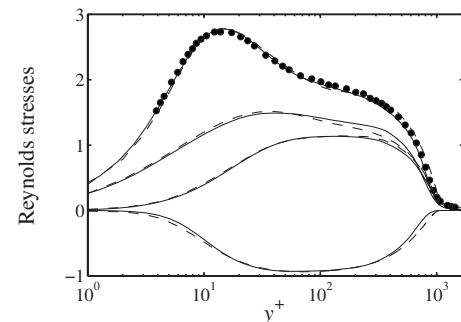


FIG. 3. Turbulent fluctuations  $u_{\text{rms}}^+$ ,  $w_{\text{rms}}^+$ ,  $u_{\text{rms}}^+$ , and shear stress  $\langle u'v' \rangle^+$  (from top). (—) Present DNS at  $Re_\theta=2512$ , (●) experiments at  $Re_\theta=2541$ . (---) Correlations based on the attached-eddy hypothesis (Refs. 14–16).

ment between DNS and the experimental data for the streamwise component is very good throughout the boundary layer. Higher-order statistics (skewness and flatness, not shown) of the streamwise fluctuations  $u'$  also show good agreement at all positions. Concerning the other velocity fluctuations and the shear stresses, the predictions from the attached-eddy hypothesis describe the present DNS data accurately.

As a side note, the pressure fluctuations close to the wall obtained from DNS (not shown) seem to scale best with a mixed scaling, yielding  $p_{w,\text{rms}}/(U_\tau \cdot U_\infty) \approx 0.112$ . In pure inner scaling, a constant increase with  $Re_\theta$  is observed, reaching  $p_{w,\text{rms}}^+ \approx 2.74$  at  $Re_\theta=2500$ , which is approximately 10% higher than for channel flow at a corresponding  $Re_\tau$ .

Averaged results give only a limited insight into the complex dynamics of the turbulent flow close to a wall. In particular, flow structures of different scales and energies are populating the near-wall and logarithmic region and contribute to the turbulent stresses. Close to the wall, the well-known turbulent streaks are the characteristic structures, essentially scaling in wall units with a length and spacing of approximately  $1000 \times 120$  wall units.<sup>17</sup> In this region, the present DNS results agree well with channel-flow data at high  $Re_\tau$ .<sup>2</sup> However, recent evidence from both experiments in pipes and boundary layers (see, e.g., Refs. 18 and 19, and the references therein), and DNS in channel flows<sup>20</sup> clearly shows that large structures, scaling in outer units, are also present. These structures reach their maximum amplitude in the overlap region, but they penetrate into the buffer layer and might even contribute to a modulation of the near-wall streaks.<sup>21</sup> Evidence from experiments and channel DNS suggests that the scaling of the large structures might be different for the various canonical flow cases, e.g., channel and boundary-layer flows. As the scale separation between inner and outer scaling is given by the Reynolds number  $Re_\tau$ , such larger structures are more easily detected at higher  $Re_\theta$ . For a quantification of the large-scale influence on the wall dynamics, we consider the fluctuating streamwise wall-shear stress  $\tau_w$ . The fluctuation amplitude  $\tau_w'/\tau_w$  is approximately 0.42 at  $Re_\theta=2500$ , in good agreement with DNS and experimental data from channel and boundary-layer flows at similar  $Re_\tau$ .<sup>22</sup> The normalized spanwise two-point correlation  $R_{\tau\tau}$  is shown in Fig. 4. This correlation indicates the spanwise spacing of the dominant (streamwise) structures at the wall. The inner peak, corresponding to the near-wall streaks,<sup>17</sup> can clearly be

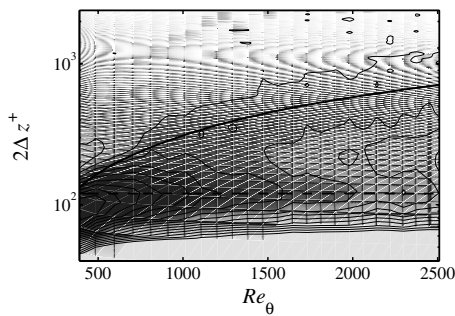


FIG. 4. Spanwise two-point correlation  $R_{\tau\tau}$  of the wall-shear stress  $\tau_w$ , computed from DNS. The spanwise axis is scaled by the displacement  $2\Delta z^+$  to show the spanwise pattern spacing. (—) corresponds to  $0.85\delta_{99}$ , (---) to  $120\ell_*$ . Shades range from dark ( $R_{\tau\tau} \leq -0.06$ ) to light ( $R_{\tau\tau} \geq 0.06$ ); contour lines go from  $-0.15$  to  $0.15$  with spacing  $0.02$ .

seen with a spacing of about 120 (local) wall units, as the first minimum of  $R_{\tau\tau}$  at  $2\Delta z^+ \approx 120$  (dashed line in Fig. 4). However, a second peak (solid line) scaling as  $2\Delta z \approx 0.85\delta_{99}$  is clearly visible in the two-point correlation for higher  $Re_\theta$ , indicating the footprint of the large-scale structures onto the fluctuating wall-shear stress. Similar observations have also been made in channel-flow simulations by Abe *et al.*<sup>23</sup> For  $Re_\theta < 1000$ , the two peaks merge into one and no clear separation is present. However, for  $Re_\theta > 1500$  two distinct peaks can be observed. Note that for these  $Re_\theta$  the outer peak is more dominant in terms of the correlation  $R_{\tau\tau}$ . These results show for the first time numerical evidence of these structures at the wall for a continuously increasing Reynolds number. It further highlights the fact that at least  $Re_\theta \approx 1500$  is needed for a sufficient separation of the inner and outer spanwise peaks. Additionally, in agreement with boundary-layer measurements,<sup>19</sup> strong maxima of the streamwise velocity spectra related to the outer peak are reached at a wall-normal distance of approximately  $0.15\delta_{99}$  and  $0.4\delta_{99}$  when scaled with either  $U_\tau^2$  or the local  $u_{rms}^2$ , respectively. The inner peak is consistently found at a wall-normal distance of  $y^+ \approx 15$  (see, e.g., Ref. 20).

In the present letter, new simulations and experiments pertaining to the important canonical flow case of a spatially developing turbulent boundary layer under zero-pressure gradient are presented up to  $Re_\theta = 2500$ . The laminar Blasius inflow in the simulations is located at  $Re_\theta = 174$ , and a localized trip forcing shortly after the inflow is causing rapid transition to turbulence similarly to the experiments. The spatial evolution of the boundary layer can be tracked over a large streamwise extent. Excellent agreement of both mean and fluctuating quantities is achieved, greatly reducing the uncertainty of boundary-layer statistics at the low to medium Reynolds numbers considered. The close agreement further validates that the results are insensitive to, e.g., the details of surface roughness, tripping device, streamwise pressure gradients, and boundary conditions. Thus, a generic zero-pressure-gradient turbulent boundary layer is recovered in both cases, which allows for a careful comparison. A first quantification of the turbulent flow structures close to the wall is presented in terms of two-point correlations of the wall-shear stress. It is seen that the boundary layer is dominated by large structures with sizes on the order of the

boundary-layer thickness that extend from the free stream down to the wall. At the wall, these structures are even more clearly visible in the fluctuating wall-shear stress than the well-known near-wall turbulent streaks, indicating that these large-scale structures might play a significant role for, e.g., the skin friction.

Computer time was provided by the Swedish National Infrastructure for Computing (SNIC). Support by the Swedish Research Council (VR) is gratefully acknowledged.

- <sup>1</sup>J. M. Österlund, A. V. Johansson, H. M. Nagib, and M. H. Hites, "A note on the overlap region in turbulent boundary layers," *Phys. Fluids* **12**, 1 (2000).
- <sup>2</sup>S. Hoyas and J. Jiménez, "Scaling of the velocity fluctuations in turbulent channels up to  $Re_\tau = 2003$ ," *Phys. Fluids* **18**, 011702 (2006).
- <sup>3</sup>X. Wu and P. Moin, "A direct numerical simulation study on the mean velocity characteristics in turbulent pipe flow," *J. Fluid Mech.* **608**, 81 (2008).
- <sup>4</sup>P. R. Spalart, "Direct simulation of a turbulent boundary layer up to  $Re_\theta = 1410$ ," *J. Fluid Mech.* **187**, 61 (1988).
- <sup>5</sup>J. Komminaho and M. Skote, "Reynolds stress budgets in Couette and boundary layer flows," *Flow, Turbul. Combust.* **68**, 167 (2002).
- <sup>6</sup>A. Ferrante and S. Elghobashi, "Reynolds number effect on drag reduction in a microbubble-laden spatially developing turbulent boundary layer," *J. Fluid Mech.* **543**, 93 (2005).
- <sup>7</sup>A. Honkan and Y. Andreopoulos, "Vorticity, strain-rate and dissipation characteristics in the near-wall region of turbulent boundary layers," *J. Fluid Mech.* **350**, 29 (1997).
- <sup>8</sup>M. Chevalier, P. Schlatter, A. Lundbladh, and D. S. Henningson, "SIMSON—A pseudo-spectral solver for incompressible boundary layer flows," KTH Stockholm Technical Report No. TRITA-MEK 2007:07, Stockholm, Sweden, 2007.
- <sup>9</sup>J. M. Österlund, "Experimental studies of zero pressure-gradient turbulent boundary-layer flow," Ph.D. thesis, KTH Stockholm, 1999.
- <sup>10</sup>A. V. Johansson and P. H. Alfredsson, "Effects of imperfect spatial resolution on measurements of wall-bounded turbulent shear flows," *J. Fluid Mech.* **137**, 409 (1983).
- <sup>11</sup>J. D. Rüedi, H. M. Nagib, J. M. Österlund, and P. A. Monkewitz, "Evaluation of three techniques for wall-shear stress measurements in three-dimensional flows," *Exp. Fluids* **35**, 389 (2003).
- <sup>12</sup>W. M. Kays and M. E. Crawford, *Convective Heat and Mass Transfer*, 3rd ed. (McGraw-Hill, New York, 1993).
- <sup>13</sup>P. A. Monkewitz, K. A. Chauhan, and H. M. Nagib, "Self-consistent high-Reynolds-number asymptotics for zero-pressure-gradient turbulent boundary layers," *Phys. Fluids* **19**, 115101 (2007).
- <sup>14</sup>I. Marusic and G. J. Kunkel, "Streamwise turbulence intensity formulation for flat-plate boundary layers," *Phys. Fluids* **15**, 2461 (2003).
- <sup>15</sup>G. J. Kunkel and I. Marusic, "Study of the near-wall-turbulent region of the high-Reynolds-number boundary layer using an atmospheric flow," *J. Fluid Mech.* **548**, 375 (2006).
- <sup>16</sup>A. E. Perry, I. Marusic, and M. B. Jones, "On the streamwise evolution of turbulent boundary layers in arbitrary pressure gradients," *J. Fluid Mech.* **461**, 61 (2002).
- <sup>17</sup>S. J. Kline, W. C. Reynolds, F. A. Schraub, and P. W. Runstadler, "The structure of turbulent boundary layers," *J. Fluid Mech.* **30**, 741 (1967).
- <sup>18</sup>K. C. Kim and R. J. Adrian, "Very large-scale motion in the outer layer," *Phys. Fluids* **11**, 417 (1999).
- <sup>19</sup>N. Hutchins and I. Marusic, "Evidence of very long meandering features in the logarithmic region of turbulent boundary layers," *J. Fluid Mech.* **579**, 1 (2007).
- <sup>20</sup>J. C. del Álamo and J. Jiménez, "Spectra of the very large anisotropic scales in turbulent channels," *Phys. Fluids* **15**, L41 (2003).
- <sup>21</sup>N. Hutchins and I. Marusic, "Large-scale influences in near-wall turbulence," *Philos. Trans. R. Soc. London, Ser. A* **365**, 647 (2007).
- <sup>22</sup>P. H. Alfredsson, A. V. Johansson, J. H. Haritonidis, and H. Eckelmann, "The fluctuating wall-shear stress and the velocity field in the viscous sublayer," *Phys. Fluids* **31**, 1026 (1988).
- <sup>23</sup>H. Abe, H. Kawamura, and H. Choi, "Very large-scale structures and their effects on the wall shear-stress fluctuations in a turbulent channel flow up to  $Re_\tau = 640$ ," *ASME J. Fluids Eng.* **126**, 835 (2004).